Fermionic Symmetry-Protected Topological Phase in a Two-Dimensional Hubbard Model

Cheng-Chien Chen,[1,2] Lukas Muechler,[3] Roberto Car,[3] Titus Neupert,[4] and Joseph Maciejko[5,6,7]
[1]Advanced Photon Source, Argonne National Laboratory, Argonne, Illinois 60439, USA
[2]Department of Physics, University of Alabama at Birmingham, Birmingham, Alabama 35294, USA
[3]Department of Chemistry, Princeton University, Princeton, New Jersey 08544, USA
[4]Princeton Center for Theoretical Science, Princeton University, Princeton, New Jersey 08544, USA
[5]Department of Physics, University of Alberta, Edmonton, Alberta T6G 2E1, Canada
[6]Theoretical Physics Institute, University of Alberta, Edmonton, Alberta T6G 2E1, Canada
[7]Canadian Institute for Advanced Research, Toronto, Ontario M5G 1Z8, Canada
(Received 4 April 2016; published 25 August 2016)

We study the two-dimensional (2D) Hubbard model using exact diagonalization for spin-1/2 fermions on the triangular and honeycomb lattices decorated with a single hexagon per site. In certain parameter ranges, the Hubbard model maps to a quantum compass model on those lattices. On the triangular lattice, the compass model exhibits collinear stripe antiferromagnetism, implying d-density wave charge order in the original Hubbard model. On the honeycomb lattice, the compass model has a unique, quantum disordered ground state that transforms nontrivially under lattice reflection. The ground state of the Hubbard model on the decorated honeycomb lattice is thus a 2D fermionic symmetry-protected topological phase. This state—protected by time-reversal and reflection symmetries—cannot be connected adiabatically to a free-fermion topological phase.

DOI: 10.1103/PhysRevLett.117.096405

Introduction.—The discovery of topological band insulators (TBIs) of noninteracting electrons in certain strongly spin-orbit coupled semiconductors is one of the most important advances of the last decade in condensed matter physics [1]. TBIs are an example of symmetry-protected topological (SPT) phases [2], which are devoid of intrinsic topological order such as that found in fractional quantum Hall systems, but possess protected edge or surface states with exotic characteristics. A major focus of current research is to discover interacting SPT phases that cannot be adiabatically deformed into noninteracting TBIs. While progress has been made in the classification [3–7] and theoretical realization in model Hamiltonians [8–13] of SPT phases of bosons, much less is known about SPT phases of fermions, which are relevant for electrons in solids. Although recent theories suggest that fermionic SPT phases distinct from free-fermion TBIs should exist in principle [14,15], apart from the special case of one spatial dimension (1D) there has been no explicit realization of a fermionic SPT phase as the ground state of a microscopic model Hamiltonian. In this Letter, we provide evidence that a 2D fermionic SPT phase protected by time-reversal and reflection symmetries and distinct from a free-fermion TBI can be realized as the ground state of a simple Hubbard model for spin-1/2 electrons on a decorated honeycomb lattice.

Fermionic Hubbard model.—We consider the Hubbard model for spin-1/2 fermions hopping on the decorated triangular and honeycomb lattices (Fig. 1), where each site $\mathbf{R}$ of the original triangular and honeycomb lattices is decorated by a single hexagon. Fermions hop within each hexagon with a nearest-neighbor amplitude t and a next-nearest-neighbor amplitude t_2, and interact via an on-site repulsion $U > 0$; hopping between the hexagons proceeds with an amplitude t'. The local Hamiltonian $\mathcal{H}_{\hexagon}^{\mathbf{R}}$ for a hexagon on site $\mathbf{R}$ is

$$\mathcal{H}_{\hexagon}^{\mathbf{R}} = -\sum_{\sigma}\sum_{i=1}^{6}(t c_{\mathbf{R}i\sigma}^{\dagger} c_{\mathbf{R},i+1,\sigma} + t_2 c_{\mathbf{R}i\sigma}^{\dagger} c_{\mathbf{R},i+2,\sigma} + \text{H.c.}) + U\sum_{i=1}^{6} n_{\mathbf{R}i\uparrow} n_{\mathbf{R}i\downarrow}, \tag{1}$$

where $c_{\mathbf{R}i\sigma}^{\dagger}$ ($c_{\mathbf{R}i\sigma}$) creates (annihilates) a fermion of spin σ on the ith vertex of the hexagon at $\mathbf{R}$, and $n_{\mathbf{R}i\sigma} \equiv c_{\mathbf{R}i\sigma}^{\dagger} c_{\mathbf{R}i\sigma}$

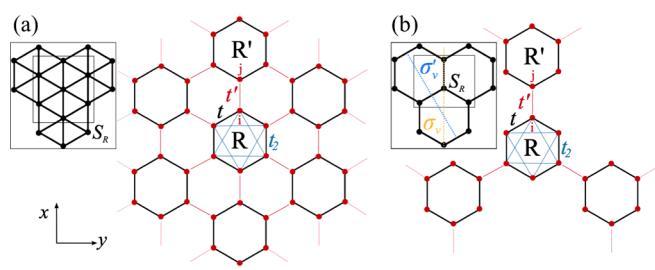

FIG. 1. Hubbard model on (a) the decorated triangular lattice and (b) the decorated honeycomb lattice. Each site of the undecorated lattice is replaced by a six-site hexagon with an intrahexagon nearest-neighbor hopping amplitude t and a next-nearest-neighbor hopping amplitude t_2; the hexagons are connected by an interhexagon nearest-neighbor hopping amplitude t'.

 © 2016 American Physical Society

is the fermion number operator. We define $c_{\mathbf{R},i+6,\sigma} \equiv c_{\mathbf{R}i\sigma}$, corresponding to periodic boundary conditions within the hexagon. We study the model at half filling with six fermions on each hexagon. The full Hamiltonian on the decorated lattice is then

$$\mathcal{H} = \sum_{\mathbf{R}} \mathcal{H}_{\hexagon}^{\mathbf{R}} - t' \sum_{\langle \mathbf{R}i,\mathbf{R}'j\rangle,\sigma} (c_{\mathbf{R}i\sigma}^{\dagger} c_{\mathbf{R}'j,\sigma} + \mathrm{H.c.}), \qquad (2)$$

where the sum in the second term runs over pairs of nearest-neighbor hexagons located at $\mathbf{R}, \mathbf{R}'$, and i, j are nearest-neighbor sites on the two adjacent hexagons (Fig. 1). The Hamiltonian possesses $SU(2)$ spin rotation symmetry, time-reversal (T) symmetry, and the C_{6v} point group symmetry of the triangular Bravais lattice.

We wish to investigate the ground state properties of Eq. (2) in the limit of weakly coupled hexagons, $t' \to 0$. For $t' = 0$, the hexagons are decoupled and the many-body ground state is simply the product of the ground states of isolated hexagons. As shown previously [16], for $t_2 > t$ in a certain range of U, the ground state of an isolated hexagon is doubly degenerate and transforms as the E_2 irreducible representation of C_{6v}, whose two components have $d_{x^2-y^2}$ and d_{xy} symmetry, respectively [17]. This ground state doublet is separated from the excited states by a finite energy gap Δ. The ground state of Eq. (2) for $t' = 0$ thus has a macroscopic degeneracy of 2^N, where N is the total number of sites of the (undecorated) triangular or honeycomb lattice. Our strategy is to lift this macroscopic degeneracy by weakly coupling these strongly correlated hexagons with a nonzero infinitesimal t', in the hope of uncovering interesting ground states for the full Hamiltonian (2). The rest of the Letter assumes the values $U/t = 8$ and $t_2/t = 1.8$, corresponding to the E_2 ground state for each isolated hexagon [16].

The doubly degenerate E_2 ground states of an isolated hexagon at $\mathbf{R}$ define a pseudospin-1/2 degree of freedom $\mathbf{S}_{\mathbf{R}}$, with $S_{\mathbf{R}}^z = \pm 1/2$ corresponding to the complex linear combination $d_{xy} \pm i d_{x^2-y^2}$. This pseudospin thus can be interpreted as an orbital degree of freedom. In the limit $t'/\Delta \ll 1$, the macroscopic degeneracy of the decoupled hexagon problem is lifted by virtual hopping processes between the hexagons, and an effective Hamiltonian for the degenerate ground subspace can be derived by perturbation theory in powers of t'/Δ. This effective Hamiltonian becomes a spin model for the pseudospin-1/2 degrees of freedom $\mathbf{S}_{\mathbf{R}}$ and, to leading order, is given by the quantum compass model [18],

$$\mathcal{H}_{\mathrm{S}} = \frac{J}{2} \sum_{\langle \mathbf{R}\mathbf{R}'\rangle} [\mathbf{S}_{\mathbf{R}} \cdot (\mathbf{R} - \mathbf{R}')][\mathbf{S}_{\mathbf{R}'} \cdot (\mathbf{R} - \mathbf{R}')], \qquad (3)$$

where the effective exchange coupling $J \sim (t')^2/\Delta > 0$ is antiferromagnetic and the sum is over pairs of nearest-neighbor sites on the (undecorated) triangular and honeycomb lattice. From the point of view of ground state properties, the mapping from the fermionic Hubbard model (2) to the effective spin Hamiltonian (3) is asymptotically exact in the $t' \to 0$ limit. Further, apart from the overall energy scale, Hamiltonian (3) is independent of the exact values of the parameters t_2/t and U/t so long as the individual hexagons are in the E_2 phase and $t'/\Delta \ll 1$. Our approach is to solve the spin model by exact diagonalization (ED) and determine the exact ground state for the fermionic problem in this limit [18]. The physical symmetries of the fermionic model are implemented in unusual ways in the spin model: while the Hubbard model (2) exhibits spin $SU(2)$ symmetry for the fermions, the effective spin model (3) does not preserve either pseudospin $SU(2)$ or $U(1)$ symmetry. T symmetry only flips the sign of the out-of-plane component $S_{\mathbf{R}}^z$ in Eq. (3), but not the in-plane components $S_{\mathbf{R}}^x, S_{\mathbf{R}}^y$. Furthermore, $T^2 = 1$ due to the even number of fermions on each hexagon. A C_6 spatial rotation in the fermionic model is implemented in the spin model as a simultaneous in-plane rotation of the lattice and the pseudospin operators. Apart from its connection to our fermionic problem, a solution of the compass model (3) on the triangular and honeycomb lattices is interesting in its own right, given the relevance of this model to a host of physical systems ranging from spin-orbit coupled Mott insulators to ultracold atomic gases [22].

Triangular lattice.—Previous studies have considered the compass model (3) on the triangular lattice in the semiclassical limit of large spins. The classical ground states were found to be sixfold degenerate and correspond to collinear stripe in-plane antiferromagnetic order as depicted in Fig. 2(a) [23–25]. Here, we study whether the classical orders are stable against quantum fluctuations by solving Eq. (3) with ED on N-site clusters ($N = 16$, 20, 24, 32) under periodic boundary conditions. The cluster shapes are chosen to be compatible with the classical ordering patterns while preserving a maximal amount of point group symmetries [18]. We begin by studying the static spin structure factor:

$$S_N^{\alpha\beta}(\mathbf{Q}) = \frac{1}{N^2} \sum_{\mathbf{R}\mathbf{R}'} e^{i\mathbf{Q}\cdot(\mathbf{R}-\mathbf{R}')} \langle S_{\mathbf{R}}^{\alpha} S_{\mathbf{R}'}^{\beta} \rangle. \qquad (4)$$

For all the cluster sizes under study, the in-plane component $S_N^{\parallel}(\mathbf{Q}) = S_N^{xx}(\mathbf{Q}) + S_N^{yy}(\mathbf{Q})$ always peaks at the M points [Fig. 1(c)] and dominates over the out-of-plane component $S_N^{zz}(\mathbf{Q})$. In addition, examining the individual components of $S_N^{\parallel}(\mathbf{Q})$ reveals that the spins are mainly aligned parallel to the ordering vector $\mathbf{Q}$. These results indicate the ground state indeed exhibits the type of magnetic order expected classically. In particular, finite-size scaling with $S_N^{\parallel}(M) = m_\infty^2 + (\alpha/N) + \mathcal{O}(1/N^2)$ renders a finite, positive value of $m_\infty \simeq 0.28$, which is reduced by roughly 44% from its classical value by quantum fluctuations. We also note that

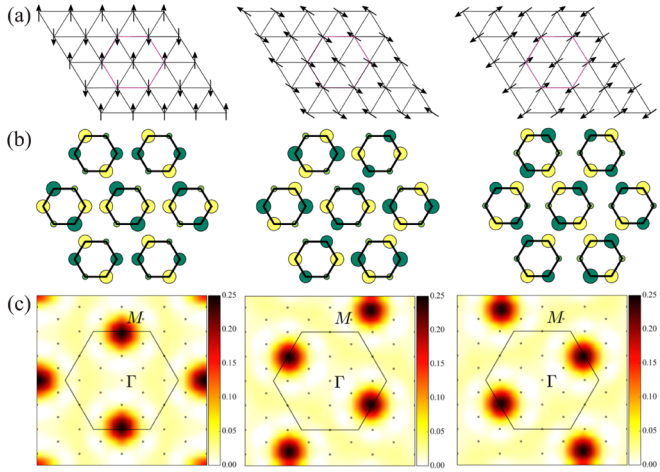

FIG. 2. (a) Classical ground states of the compass model (3) on the triangular lattice. (b) Schematics of three different degenerate fermionic quantum ground states of the Hubbard model (2). The size of the circles at each site corresponds to the deviation of the electron density from half filling. Yellow colors correspond to a surplus and green colors to a deficit. (c) In-plane static structure factors $S^{\parallel}_{N=16}(\mathbf{Q})$ of the corresponding ground states in the compass model. The results were obtained by interpolating data on the available momentum points (indicated by black dots).

the energy splitting between the two states lowest in energy decreases exponentially with cluster size as $e^{-\sqrt{N}/\xi}$, indicative of ground state degeneracy. The (sixfold) degenerate ground states are separated from the rest of the spectrum by a finite excitation gap extrapolated to be larger than $0.5J$ in the thermodynamic limit [18].

Using the mapping between pseudospins and E_2 states of the fermionic hexagonal plaquettes, one can infer the nature of the ground states of the 2D Hubbard model (2) from the magnetically ordered ground states of the pseudospin Hamiltonian (3). If out-of-plane ferromagnetic pseudospin order were to occur, this would correspond to a translationally invariant but T-breaking state of fermions with uniform $d_{xy} \pm i d_{x^2-y^2}$ order. This state would also break rotational symmetry spontaneously due to the nontrivial $e^{\pm 2\pi i/3}$ eigenvalue of the $S^z_{\mathbf{R}}$ eigenstates under C_6 rotations. However, the pseudospin in-plane antiferromagnetic order found here does not break the physical T symmetry of the original fermion problem, as the in-plane pseudospin components are even under T. Indeed, the state of a single hexagon at $\mathbf{R}$ with in-plane pseudospin forming an angle $\phi_{\mathbf{R}}$ with the x axis is given by $|\phi_{\mathbf{R}}\rangle = (|\uparrow\rangle + e^{i\phi_{\mathbf{R}}}|\downarrow\rangle)/\sqrt{2}$ in the $S^z_{\mathbf{R}}$ basis. This state corresponds to the real, and thus T-invariant, linear combination $\cos(\phi_{\mathbf{R}}/2)d_{xy} + \sin(\phi_{\mathbf{R}}/2)d_{x^2-y^2}$. To characterize how translation symmetry is broken, we calculate the density deviation from half filling $\delta n_{\mathbf{R}i}(\phi) \equiv \langle \phi_{\mathbf{R}} | \sum_\sigma n_{\mathbf{R}i\sigma} - 1 | \phi_{\mathbf{R}} \rangle$ for each of the six classical ground states, in which the pseudospin angles are $\phi_{\mathbf{R}} = (2m+1)\pi/6$, $m = 0, \ldots, 5$. As depicted schematically in Fig. 2(b), the resulting charge order in the fermion problem corresponds to a T-invariant d-density wave charge order [26] that doubles the unit cell.

Honeycomb lattice.—Semiclassical studies of the compass model on the honeycomb lattice have established the existence of a macroscopic number of classical ground states [24,25,27]; the model is thus frustrated. Whether and, if so, how the quantum model for spin-1/2 degrees of freedom orders at zero temperature is still under debate. Linear spin-wave theories predict that quantum order-by-disorder effects favor in-plane Néel order [24] or the so-called six-site plaquette order [25]. An earlier ED study on clusters up to $N = 24$ sites [27] finds a quantum disordered ground state with gapless excitations, although finite-size extrapolation cannot distinguish between gapless excited states and degenerate ground states. Furthermore, certain cluster geometries employed in that study frustrate the six-site plaquette order and thus introduce a bias. A recent tensor network study [28] suggests that the ground state develops the six-site plaquette order. Tensor network algorithms have the advantage over ED that they can be formulated directly in the thermodynamic limit, but are intrinsically variational as one assumes that the ground-state wave function can be expressed as a network of local tensors defined on each lattice site. Here, we use ED to study the 120° quantum compass model on the honeycomb lattice, as in Ref. [27], but with larger cluster sizes ($N = 18$, 24, 30, 36) and geometries that support both the Néel and six-site plaquette orders [18]. While not all the clusters we consider preserve the full C_{6v} point group, they all contain a C_{2v} subgroup with a C_2 rotation axis and two mirror planes σ_v, σ'_v [see Fig. 1(b)]. Without pseudospin $SU(2)$ and $U(1)$ symmetries in Eq. (3), the $N = 36$ calculation using translation symmetry corresponds to a Hamiltonian matrix of $\sim 3.8 \times 10^9$ basis states.

Figure 3 shows the finite-size scaling of the ground state energy and the many-body gap to the first excited state. In spin-wave theory, the ground-state energy per lattice site E_0/N is $-0.225J$. The previous ED study with $N \leq 24$ reports $E_0/N = -0.215J$ and a vanishing pseudospin gap [27]. For clusters of the same size, we obtain a lower ground-state energy due to the higher spatial symmetry of our clusters, which can accommodate both the Néel and six-site plaquette orders. In addition, while the gap decreases rapidly with increasing N for $N < 18$, it tends to saturate above $N = 18$. A linear $1/N$ extrapolation of our ED results with $N \geq 18$ yields $E_0/N = -0.222J$ (lower than the tensor-network result of $-0.148J$ [28]) and a finite excitation gap $\sim 0.05J$ in the thermodynamic limit (Fig. 3).

For all clusters, the out-of-plane structure factor $S^{zz}_N(\mathbf{Q})$ peaks at the Γ point [Fig. 4(b)], corresponding to short-range Néel order (or ferromagnetic order after a sublattice basis rotation). However, $S^{zz}_N(\Gamma)$ decreases faster than $1/N$. Both quadratic $1/N$ scaling for $N \geq 18$ and linear $1/N$ scaling for $N \geq 24$ lead to an extrapolated $S^{zz}_{N=\infty}(\Gamma) < 0$, which thereby rules out long-range Néel order in the

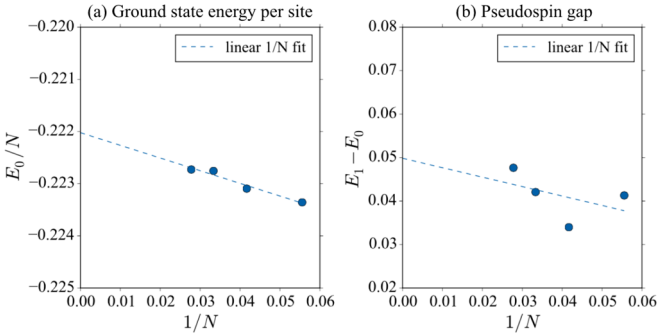

FIG. 3. Exact diagonalization energy spectra of the compass model (3) on the honeycomb lattice: (a) ground-state energy per lattice site E_0/N. All ground states reside in the zero-momentum sector. A linear $1/N$ extrapolation yields $E_0/N \sim -0.222J$ in the thermodynamic limit. (b) Energy gap above the ground state. A linear $1/N$ extrapolation yields a finite pseudospin gap $\sim 0.05J$ in the thermodynamic limit.

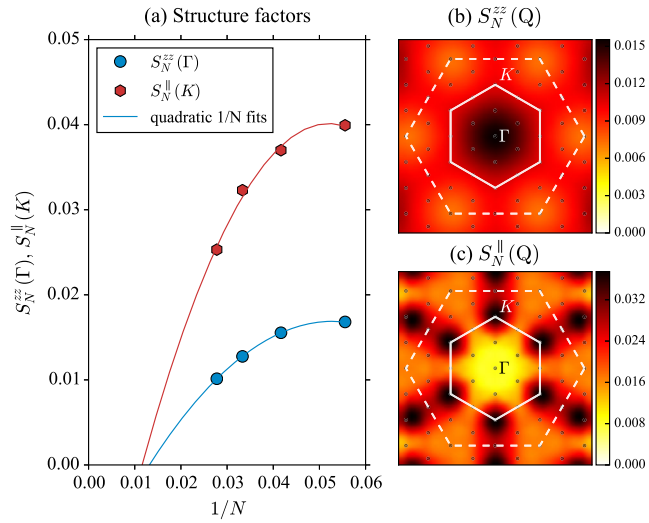

FIG. 4. Static structure factors obtained by exact diagonalization of the compass model (3) on the honeycomb lattice: (a) scalings of $S^{zz}(\mathbf{Q}=\Gamma)$ and $S^{\parallel}(\mathbf{Q}=K)$. The results show the absence of Néel and six-site plaquette orders, respectively. (b),(c) Maps of $S^{zz}_{N=24}(\mathbf{Q})$ and $S^{\parallel}_{N=24}(\mathbf{Q})$ obtained by interpolating data on the available momentum points (indicated by black dots). The first and second Brillouin zones are denoted by the solid and dashed white hexagons, respectively.

thermodynamic limit [Fig. 4(a)]. On the other hand, the in-plane structure factor $S_N^{\parallel}(\mathbf{Q})$ peaks at the K points [Fig. 4(c)], reminiscent of a short-range six-site plaquette order. $S^{\parallel}_{N=\infty}(K)$, however, also extrapolates to a negative value in the thermodynamic limit [Fig. 4(a)]. The pseudospin correlation length is estimated to be less than one unit-cell length based on the structure factor [29]. Our results thus suggest that long-range six-site plaquette order is also absent, and the ground state of the 120° compass model on the honeycomb lattice is a quantum pseudospin liquid. Because the honeycomb lattice has two sites per unit cell, according to the generalized Hastings-Oshikawa-Lieb-Schultz-Mattis theorem [30], a gapped ground state without symmetry breaking does not imply intrinsic topological order with long-range entanglement [31,32]. Since we find a unique ground state on the torus (as periodic boundary conditions are employed in both directions), we conclude that the ground state of the compass model—and thus that of the fermionic Hubbard model—are short-range entangled.

A gapped, symmetric, short-range entangled ground state for the fermionic Hubbard model (2) is either adiabatically connected to a free-fermion trivial band insulator, a free-fermion TBI, or a fermionic SPT phase distinct from the latter. To distinguish between the three, we classify the ground states of the compass model (3) according to irreducible representations of the cluster point group C_{2v}. Indeed, the ground state of a T-invariant free-fermion band insulator, trivial or topological, must transform according to the identity representation of the point group [33]. For an adiabatic path that preserves T and point group symmetries, a ground state belonging to a nontrivial 1D point-group representation cannot be adiabatically connected to a free-fermion ground state and is thus a fermionic SPT phase protected by those symmetries. On clusters with $N/2$ even, the ground state of the compass model—and thus that of the corresponding Hubbard model—belongs to the identity representation of C_{2v} and cannot be distinguished from a band insulator by its transformation properties under point group symmetries alone. With $N/2$ odd, the ground state is odd under the reflections σ_v and σ_v' indicated by the dotted lines in Fig. 1(b) and even under C_2 rotation: it thus transforms according to the A_2 representation of the C_{2v} point group and cannot be adiabatically connected to a band insulator. (See Refs. [34–36] for a tensor-network construction of a state with similar transformation properties.) In the thermodynamic limit $N \to \infty$, a band insulator would transform trivially under all point group operations for both $N/2$ odd and $N/2$ even, i.e., independently of how the thermodynamic limit is approached. Our results therefore suggest that the ground state of the fermionic Hubbard model (2) on the decorated honeycomb lattice realizes a 2D fermionic SPT phase distinct from a free-fermion TBI and protected by T and C_{2v} symmetries. Our results hold in the asymptotic limit $t' \to 0$ for a finite range of U and t_2 so long as individual hexagons are in the E_2 phase [16].

Concluding remarks.—Our numerical ED results suggest that a simple 2D Hubbard model of spin-1/2 electrons exhibits d-density wave charge order on the decorated triangular lattice but produces an interacting fermionic SPT phase distinct from a free-fermion TBI on the decorated honeycomb lattice. Given the relative simplicity of our model Hamiltonian, we expect our findings to assist in the experimental search for SPT phases of electrons in real materials. Our study is conceptually similar to that of the checkerboard Hubbard model on the square lattice, in

which isolated square plaquettes with strongly correlated ground states transforming as the B_1 ($d_{x^2-y^2}$) representation of C_{4v} couple weakly and form an exotic ground state for the entire system, the d-Mott insulator [33,37,38], which also belongs to the B_1 representation. While this is also strictly speaking a fermionic SPT phase (protected by T and C_{4v} symmetries), it is adiabatically connected to a product state of decoupled plaquettes occupying the sites of a decorated square lattice. Because C_{4v} acts on such plaquettes as an on-site symmetry of this lattice, the d-Mott insulator can be viewed as a "stack" of 0D SPT phases protected by on-site symmetries (T and C_{4v}) and the translation symmetry of the decorated lattice, i.e., as a weak SPT phase in the sense of Refs. [6,39]. By contrast, the ground state found here cannot be reduced to a product state of N hexagonal plaquettes in the A_2 representation, as such a product state would transform trivially under σ_v with eigenvalue $(-1)^N = 1$ since N is even on the honeycomb lattice, irrespective of whether $N/2$ is even or odd. Since the protecting C_{2v} symmetry of our state generally does not act as an on-site symmetry, except in the (excluded) case of a product state of 0D SPT phases, we believe our state cannot be a weak SPT phase.

The authors acknowledge discussions with B. Bauer, K. Penc, H.-C. Jiang, and T. F. Seman. C.-C. C. was supported by the Aneesur Rahman Postdoctoral Fellowship at Argonne National Laboratory, operated by the U.S. Department of Energy (DOE) under Contract No. DE-AC02-06CH11357. L. M. and R. C. were supported by U.S. DOE Contract No. DE-FG02-05ER46201. J. M. was supported by NSERC Grant No. RGPIN-2014-4608, the Canada Research Chair Program (CRC), the Canadian Institute for Advanced Research (CIFAR), and the University of Alberta. This research used resources of the National Energy Research Scientific Computing Center, supported by U.S. DOE Contract No. DE-AC02-05CH11231.

[1] X.-L. Qi and S.-C. Zhang, Phys. Today, **63**, No. 1, 33 (2010).
[2] T. Senthil, Annu. Rev. Condens. Matter Phys. **6**, 299 (2015).
[3] Z.-C. Gu and X.-G. Wen, Phys. Rev. B **80**, 155131 (2009).
[4] F. Pollmann, E. Berg, A. M. Turner, and M. Oshikawa, Phys. Rev. B **85**, 075125 (2012).
[5] X. Chen, Z.-X. Liu, and X.-G. Wen, Phys. Rev. B **84**, 235141 (2011).
[6] X. Chen, Z.-C. Gu, Z.-X. Liu, and X.-G. Wen, Phys. Rev. B **87**, 155114 (2013).
[7] X. Chen, Z.-C. Gu, Z.-X. Liu, and X.-G. Wen, Science **338**, 1604 (2012).
[8] M. Levin and Z.-C. Gu, Phys. Rev. B **86**, 115109 (2012).
[9] T. Senthil and M. Levin, Phys. Rev. Lett. **110**, 046801 (2013).
[10] N. Regnault and T. Senthil, Phys. Rev. B **88**, 161106 (2013).
[11] S. D. Geraedts and O. I. Motrunich, Ann. Phys. (Berlin) **334**, 288 (2013).
[12] F. J. Burnell, X. Chen, L. Fidkowski, and A. Vishwanath, Phys. Rev. B **90**, 245122 (2014).
[13] S. D. Geraedts and O. I. Motrunich, Phys. Rev. X **4**, 041049 (2014).
[14] Z.-C. Gu and X.-G. Wen, Phys. Rev. B **90**, 115141 (2014).
[15] C. Wang, A. C. Potter, and T. Senthil, Science **343**, 629 (2014).
[16] L. Muechler, J. Maciejko, T. Neupert, and R. Car, Phys. Rev. B **90**, 245142 (2014).
[17] M. Sigrist and K. Ueda, Rev. Mod. Phys. **63**, 239 (1991).
[18] See Supplemental Material at http://link.aps.org/supplemental/10.1103/PhysRevLett.117.096405, which includes Refs. [19–21], for a derivation of the compass model and further calculation details.
[19] S. Balay, W. D. Gropp, L. C. McInnes, and B. F. Smith, in *Modern Software Tools in Scientific Computing*, edited by E. Arge, A. M. Bruaset, and H. P. Langtangen (Birkhäuser Press, Boston, 1997), pp. 163–202.
[20] V. Hernandez, J. E. Roman, and V. Vidal, ACM Trans. Math. Softw. **31**, 351 (2005).
[21] G. W. Stewart, SIAM J. Matrix Anal. Appl. **23**, 601 (2002).
[22] Z. Nussinov and J. van den Brink, Rev. Mod. Phys. **87**, 1 (2015).
[23] M. V. Mostovoy and D. I. Khomskii, Phys. Rev. Lett. **89**, 227203 (2002).
[24] E. Zhao and W. V. Liu, Phys. Rev. Lett. **100**, 160403 (2008).
[25] C. Wu, Phys. Rev. Lett. **100**, 200406 (2008).
[26] C. Nayak, Phys. Rev. B **62**, 4880 (2000).
[27] J. Nasu, A. Nagano, M. Naka, and S. Ishihara, Phys. Rev. B **78**, 024416 (2008).
[28] H. Zou, B. Liu, E. Zhao, and W. V. Liu, New J. Phys. **18**, 053040 (2016).
[29] A. W. Sandvik, AIP Conf. Proc. **1297**, 135 (2010).
[30] H. Watanabe, H. C. Po, A. Vishwanath, and M. Zaletel, Proc. Natl. Acad. Sci. U.S.A. **112**, 14551 (2015).
[31] A. Kitaev and J. Preskill, Phys. Rev. Lett. **96**, 110404 (2006).
[32] M. Levin and X.-G. Wen, Phys. Rev. Lett. **96**, 110405 (2006).
[33] H. Yao and S. A. Kivelson, Phys. Rev. Lett. **105**, 166402 (2010).
[34] I. Kimchi, S. A. Parameswaran, A. M. Turner, F. Wang, and A. Vishwanath, Proc. Natl. Acad. Sci. U.S.A. **110**, 16378 (2013).
[35] B. Ware, I. Kimchi, S. A. Parameswaran, and B. Bauer, Phys. Rev. B **92**, 195105 (2015).
[36] P. Kim, H. Lee, S. Jiang, B. Ware, C.-M. Jian, M. Zaletel, J. H. Han, and Y. Ran, arXiv:1509.04358.
[37] H. Yao, W.-F. Tsai, and S. A. Kivelson, Phys. Rev. B **76**, 161104 (2007).
[38] H.-Q. Wu, R.-Q. He, Z. Y. Meng, and Z.-Y. Lu, Phys. Rev. B **91**, 125128 (2015).
[39] M. Cheng, M. Zaletel, M. Barkeshli, A. Vishwanath, and P. Bonderson, arXiv:1511.02263.